Inorg. Chem. **2006**, *45*, 2391–2393

Validity of the Classical Monte Carlo Method To Model the Magnetic Properties of a Large Transition-Metal Cluster: Mn_{19}

Nicola Lima,[†] Andrea Caneschi,[†] Dante Gatteschi,*[,†] Mikael Kritikos,[‡] and L. Gunnar Westin[§]

Department of Chemistry and UdR INSTM, University of Florence, 50019 Sesto Fiorentino, Italy, Department of Inorganic Chemistry, Ångström Laboratory, Uppsala University, 75121 Uppsala, Sweden, and Department of Structural Chemistry, Arrhenius Laboratory, Stockholm University, 10691 Stockholm, Sweden

Received November 9, 2005

The susceptibility of the large transition-metal cluster $[Mn_{19}O_{12}(MOE)_{14}(MOEH)_{10}]\cdot MOEH$ (MOE = $OC_2H_2O–CH_3$) has been fitted through classical Monte Carlo simulation, and an estimation of the exchange coupling constants has been done. With these results, it has been possible to perform a full-matrix diagonalization of the cluster core, which was used to provide information on the nature of the low-lying levels.

The development of inorganic chemistry and molecular magnetism nowadays has kept pace with the synthesis of larger and larger transition-metal clusters.[1] The increase in the size of these clusters has made the achievement of exact solutions through full-matrix diagonalization, to study the magnetic behavior, very difficult or even impossible. Alternative methods, like density functional theory techniques, have been utilized to solve the problem,[2] but the drawback is that they are very time- and resource-consuming. Simpler but equally effective methods based on classical Monte Carlo (MC) algorithms are much less demanding in terms of computer resources and have been successfully utilized in many cases to calculate the susceptibility of these systems.[3] The $[Mn_{19}O_{12}(MOE)_{14}(MOEH)_{10}]\cdot MOEH$ (MOE = $OC_2H_2O-CH_3$) cluster,[4] represented in Figure 1, made up of 19 Mn^{II} ions, is a good system for testing the goodness of this type of approach because the dimension of Hilbert's space is greater than 6×10^{14}; therefore, it is impossible to fully diagonalize the spin Hamiltonian.

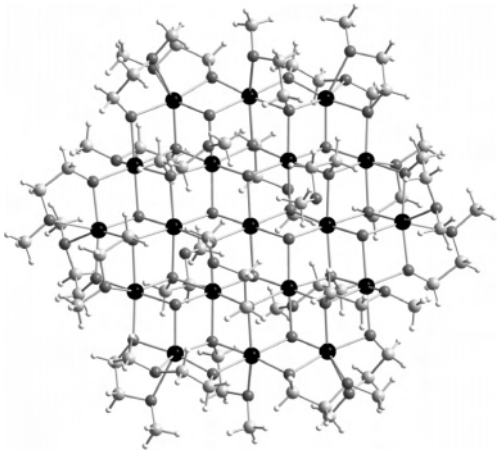

Figure 1. Diamond view of $[Mn_{19}O_{12}(MOE)_{14}(MOEH)_{10}]\cdot MOEH$. The black spheres correspond to Mn atoms, while O, C, and H atoms are represented by different shades of gray, from darker to brighter, respectively.

To rationalize the magnetic properties of $[Mn_{19}O_{12}(MOE)_{14}(MOEH)_{10}]\cdot MOEH$, the curve of the product $\chi_M T$ has been fitted by making use of a classical MC algorithm, which allows us to compute average macroscopic observables through the extraction of random numbers, combined with the MINUIT[5] minimization routine, which makes the parameters vary in order to reproduce as best as one can the experimental behavior. The details of the programs and the calculations have been reported in the Supporting Information. The system is defined by the classical spin Hamiltonian:

$$H = \sum_{i,j<i} J_{ij} \vec{S}_i \cdot \vec{S}_j \qquad (1)$$

where $S_i = [S_i(S_i + 1)]^{1/2}$ is the scaled classical module of the spin of the paramagnetic center i and J_{ij} is the isotropic exchange coupling constant between atoms i and j.

* To whom correspondence should be addressed. E-mail: dante.gatteschi@unifi.it.
† University of Florence.
‡ Stockholm University.
§ Uppsala University.

(1) (a) Müller, A.; Kögerler, P.; Dress, A. W. M. *Coord. Chem. Rev.* **2001**, *222*, 193. (b) Tasiopoulos, A. J.; Vinslava, A.; Wernsdorfer, W.; Abboud, K. A.; Christou, G. *Angew. Chem., Int. Ed.* **2004**, *43*, 2117.
(2) (a) Park, K.; Pederson, M. R.; Hellberg, C. S. *Phys. Rev. B* **2004**, *69*, 14416. (b) Hegetschweiler, K.; Morgenstern, B.; Zubieta, J.; Hagrman, P. J.; Lima, N.; Sessoli, R.; Totti, F. *Angew. Chem., Int. Ed.* **2004**, *43*, 3436. (c) Ruiz, E.; Rodríguez-Fortea, A.; Cano, J.; Alvarez, S. *J. Phys. Chem. Solids* **2004**, *65*, 799.
(3) (a) Benelli, C.; Cano, J.; Journaux, Y.; Sessoli, R.; Solan, G. A.; Winpenny, R. E. P. *Inorg. Chem.* **2001**, *40*, 188. (b) Boullant, E.; Cano, J.; Journaux, Y.; Decurtins, S.; Gross, M.; Pilkington, M. *Inorg. Chem.* **2001**, *40*, 3900.
(4) Pohl, I. A. M.; Westin, L. G.; Kritikos, M. *Chem. Eur. J.* **2001**, *7*, 3439.
(5) *MINUIT Function Minimization and Error Analysis*; CERN Program Library entry D506; CERN: Geneva, Switzerland, 1994−1998.

10.1021/ic051936h CCC: $33.50
Published on Web 03/01/2006

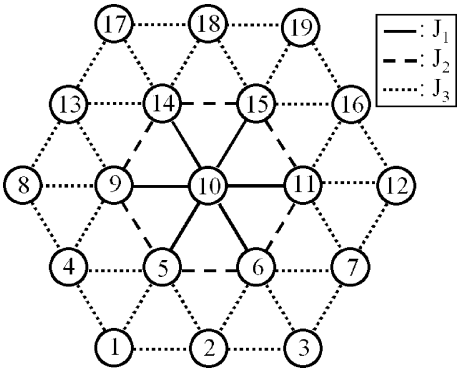

Figure 2. Atom-numbering and exchange coupling scheme between Mn ions of $[Mn_{19}O_{12}(MOE)_{14}(MOEH)_{10}]\cdot MOEH$.

The magnetic susceptibility, $\chi_M^{\alpha\alpha}$, has been obtained from the magnetization fluctuations:[6]

$$\chi_M^{\alpha\alpha} = (1/k_B T)[\langle(\sum_i \mu_i^{\alpha})^2\rangle - \langle\sum_i \mu_i^{\alpha}\rangle^2] \qquad (2)$$

where α is a space direction ($\alpha = x, y, z$), $\chi_M^{\alpha\alpha}$ is the macroscopic magnetic susceptibility, $\mu_i^{\alpha} = g_i \mu_B S_i^{\alpha}$ is the magnetic moment along α, k_B is Boltzmann's constant, g_i is the Landé factor, μ_B is the Bohr magneton, and S_i^{α} is the projection of the ith spin along α. Because (1) is isotropic, $\chi_M^{xx} \equiv \chi_M^{yy} \equiv \chi_M^{zz}$. Several simulations have been carried out with different starting conditions to find the best one and to test the reproducibility of the calculation.

Because of the fact that the system lies on a 3-fold rotoinversion axis, seven types of bridges between nearest-neighbor Mn^{II} ions have been found corresponding to seven different exchange pathways. To reduce the number of parameters, some coupling constants have been considered to be equal to each other. The strength of superexchange magnetic interactions comes from three principal factors: the nature of the bridging ligands and the distances and angles between interacting magnetic atoms. Even for ions with a high-spin d^5 configuration, the coupling constant varies with the angle.[7]

The seven different exchange interactions can be grouped into three different macro groups: one that contains symmetric bis(μ_3-oxo) bridges, another one that contains symmetric (μ_3-oxo)(μ_3-alkoxo) bridges, and the last one that contains distorted bis(μ_3-alkoxo), (μ_2-alkoxo)(μ_3-alkoxo), and (μ_3-oxo)(μ_2-alkoxo) bridges, which we refer to as J_1, J_2, and J_3, respectively. In Figure 2, the exchange coupling scheme between Mn atoms is shown. Setting the g values of all Mn^{II} ions to 2.00, a best fit through a least-squares analysis of the data has been found with $J_1 = 24$ K, $J_2 = 16$ K, and $J_3 = 3$ K, with $R = 2.1 \times 10^{-4}$, with

$$R = [\sum_{i=1}^{n}(\chi_i^{obs} - \chi_i^{calc})^2 / \sum_{i=1}^{n}(\chi_i^{obs})^2]^{1/2}/n \qquad (3)$$

where R is the agreement factor, n is the number of points considered, and χ_i^{obs} and χ_i^{calc} are the experimental and calculated magnetic susceptibilities, respectively.

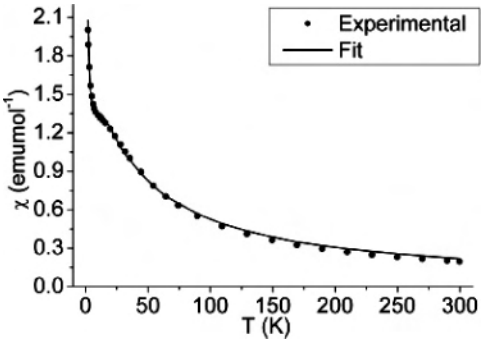

Figure 3. Experimental data (full circle) and MC calculation (line) plots of χ_M against T for $[Mn_{19}O_{12}(MOE)_{14}(MOEH)_{10}]\cdot MOEH$.

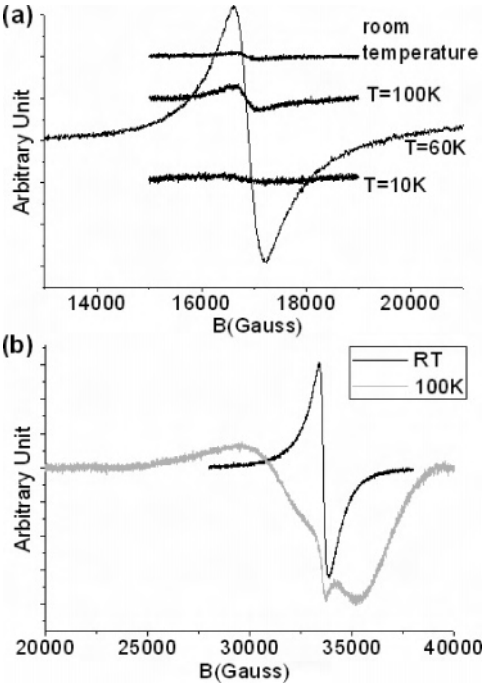

Figure 4. W-band EPR spectra of $[Mn_{19}O_{12}(MOE)_{14}(MOEH)_{10}]\cdot MOEH$: (a) low-field transition; (b) high-field transition.

In Figure 3, the best fit χ vs T curve, together with the experimental data, is shown. The interesting feature is that the shoulder at ca. 12 K is well reproduced. A good fit was also obtained for the χT vs T curve. As expected, we have found antiferromagnetic interactions between Mn^{II} ions; moreover, the strength of these interactions diminishes upon passing from symmetric bis(μ_3-oxo) bridges to distorted bis-(μ_3-alkoxo), (μ_2-alkoxo)(μ_3-alkoxo), and (μ_3-oxo)(μ_2-alkoxo) ones.

Electron paramagnetic spectra (EPR), at W-band (95-GHz) frequency, of $[Mn_{19}O_{12}(MOE)_{14}(MOEH)_{10}]\cdot MOEH$ have been recorded from room temperature to 10 K and are reported in Figure 4. We can observe two signals, one around 16 800 G and the other around 33 600 G. The low-field feature is attributed to forbidden $\Delta m_S = \pm 2$ transitions.

(6) Gould, H.; Tobochnik, J. An Introduction to Computer Simulation Methods. *Applications to Physical Systems*, 2nd ed.; Addison-Wesley: Reading, MA, 1996.

(7) Le Gall, F.; Fabrizi de Biani, F.; Caneschi, A.; Cinelli, P.; Cornia, A.; Fabretti, A. C.; Gatteschi, D. *Inorg. Chim. Acta* **1997**, *262*, 123.

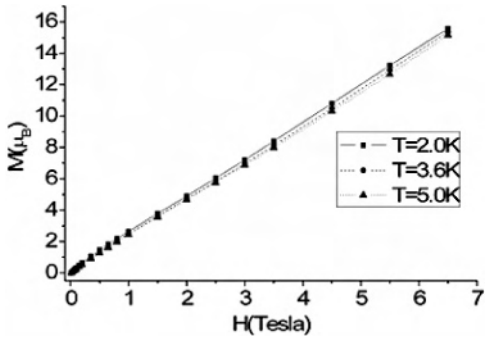

Figure 5. Field dependence of the magnetization at 2.0, 3.6, and 5.0 K of $[Mn_{19}O_{12}(MOE)_{14}(MOEH)_{10}]\cdot MOEH$.

The signal shows a continuous increase of its intensity upon a decrease in the temperature, with a maximum at around 60 K. Below this temperature, down to 10 K, the intensity decreases. This behavior suggests that there is or there are some excited states with $S > {}^1/_2$ whose population reaches a maximum at around 60 K; then they begin to depopulate as the temperature decreases. The high-field (HF) transition is an isotropic $g = 2$ signal, and it is typical for a system of strongly coupled Mn^{II} ions. In this case, the signal abruptly increases as the temperature decreases, making recording of the spectra impossible because of saturation of the detector and loss of matching of the cavity, even with high attenuation. Moreover, HF-EPR spectra at 285 GHz have been recorded from 150 to 16 K, but they have not given any new results because they show the same structure as the 95-GHz ones, i.e., a broad signal around $g = 2$ and the problem of its saturation.

The nature of the ground state is not defined by the above results, and the MC method does not help. Magnetization data in the range of 2−5 K are shown in Figure 5. The field dependence is almost linear, and no evidence of saturation is achieved. However, at 6.5 T, the magnetization reaches 15.6 μ_B, indicating that levels with $S \geq 8$ are populated. The linear dependence is indicative of the presence of a quasi-continuum of levels, as observed in an Fe30 cluster.[8]

In an attempt to gain more insight into the low-lying levels, we investigated the energy of the spin levels of the seven Mn ions of the core, that is, referring to Figure 2: Mn5, Mn6, Mn9, Mn10, Mn11, Mn14, and Mn15, which we refer to as an Mn7 cluster. In this case, it is possible to perform a full-matrix diagonalization of the reduced system, utilizing the coupling constant J_1 and J_2 obtained from the MC simulation of the whole cluster and a quantistic Hamiltonian, reported in equation S3 in the Supporting Information, together with the CLUMAG subroutine.[9] Theoretical values for the magnetization of the Mn7 cluster, in the range of 2−5 K, are shown in Figure S1 in the Supporting Information.

The first six eigenstates and eigenvalues have been reported in Table 1. From Table 1, we observe that the spin ground state for the reduced cluster is $S = {}^5/_2$ and its eigenvector could be visualized as the antiferromagnetic interaction between the central Mn^{II} ion, with $S = {}^5/_2$, and the six external Mn^{II} ions with a total spin of $S = 5$, leading to the $S = {}^5/_2$ ground state. The intermediate state $S = 5$ is stabilized by spin-frustration effects in antiferromagnetic triangles. This is in good agreement with the experimental data if we consider that, as obtained from the MC simulation, the 12 external Mn^{II} ions are weakly interacting with each other and with the strongly coupled Mn7 core.

Table 1. First Six Spin States and Their Relative Energies of the Mn7 Cluster

eigenvector $\lvert S_{5,6}S_{11,15}S_{9,14}S_{5,6,11,15}S_{5,6,11,15,9,14}S\rangle$	eigenvalue $E_{\text{ground state}} - E_{\text{excited state}}$ (cm^{-1})
$\lvert 1\,2\,2\,3\,5\,{}^5/_2\rangle$	0
$\lvert 2\,2\,2\,4\,6\,{}^7/_2\rangle$	4.6
$\lvert 1\,1\,2\,2\,4\,{}^3/_2\rangle$	6.0
$\lvert 2\,2\,3\,4\,7\,{}^9/_2\rangle$	19.8
$\lvert 1\,1\,1\,2\,3\,{}^1/_2\rangle$	22.7
$\lvert 2\,3\,3\,5\,8\,1{}^1/_2\rangle$	45.4

In this case, at high temperatures we could have a value of $\chi_M T$ resulting from 12 uncoupled Mn^{II} spins plus the contribution of the Mn7 core $\chi_M T = 0.125 g_{Mn^{II}}{}^2[12 S_{Mn^{II}}(S_{Mn^{II}} + 1) + S_{Mn7}^{\text{high } T}(S_{Mn7}^{\text{high } T} + 1)]$ with $g_{Mn^{II}} = 2.0$, $S_{Mn^{II}} = {}^5/_2$, and $S_{Mn7}^{\text{high } T} = 5$ as derived from the high-temperature value of χ of the Mn7 cluster, making use of the spin-only formula:

$$\chi = \frac{N g^2 \mu_B{}^2}{3 k_B T} S(S+1) \qquad (4)$$

which leads to $\chi_M T = 67.5$ emu K mol^{-1}, compared with the experimental value of 58.86 emu K mol^{-1}. At low temperature, antiferromagnetic interactions among the 12 external Mn^{II} ions and between them and the Mn7 core produce spin frustration in the system. If we suppose that the external ring gives a null contribution to the product $\chi_M T$, we obtain $\chi_M T = 0.125 g_{Mn^{II}}{}^2[S_{Mn7}^{\text{low } T}(S_{Mn7}^{\text{low } T} + 1)] = 4.375$ emu K mol^{-1}, with $S_{Mn7}^{\text{low } T} = {}^5/_2$, compared with the experimental value of 3.43 emu K mol^{-1}; otherwise, we should consider the coupling between all Mn atoms and, consequently, the Mn7 approximation should no longer be suitable.

In conclusion, we have fitted the experimental magnetic data of $[Mn_{19}O_{12}(MOE)_{14}(MOEH)_{10}]\cdot MOEH$ utilizing a MC algorithm together with a minimization routine. The quality of the results thus obtained confirms the goodness of MC techniques for the study of a high-nuclearity metal cluster without the need for high-performance workstations.

Acknowledgment. This work was supported by the EU under the SENTINEL program (HPRU-CT-2000-40022), MIUR, FIRB, and PRIN projects, RTN, QUEMOLNA (FP6-504880), and the Swedish Science Council (VR).

Supporting Information Available: Computational details and plot of the field dependence of the magnetization at 2.0, 3.6, and 5.0 K of Mn7. This material is available free of charge via the Internet at http://pubs.acs.org.

IC051936H

(8) (a) Müller, A.; Luban, M.; Christian, S.; Modler, R.; Kögeler, P.; Axenovich, M.; Schnack, J.; Canfield, P.; Bud'ko, S.; Harrison, N. *Chem. Phys. Chem.* **2001**, *2*, 517. (b) Axenovich, M.; Luban, M. *Phys. Rev. B* **2001**, *63*, 100407.

(9) Gatteschi, D.; Pardi, L. *Gazz. Chim. Ital.* **1993**, *123*, 231.